Field and laboratory experiments on high dissolution rates of limestone in stream flow

Tsuyoshi Hattanji[1], Mariko Ueda[2], Wonsuh Song[3], Nobuyuki Ishii[4],
Yuichi S. Hayakawa[3], Yasuhiko Takaya[3] and Yukinori Matsukura[1]

[1] Faculty of Life and Environmental Sciences, University of Tsukuba
[2] Graduate School of Life and Environmental Sciences, University of Tsukuba
[3] Center for Spatial Information Science, The University of Tokyo
[4] College of Geoscience, University of Tsukuba

Abstract

Field and laboratory experiments were performed to examine dissolution rates of limestone in stream flow. Field experiments were conducted in three stream sites (A – C) with different lithological or hydrological settings around a limestone plateau in the Abukuma Mts., Japan. Sites A and B are allogenic streams, which flow from non-limestone sources into dolines, and site C has a karst spring source. Tablets made of limestone from the same plateau with a diameter of 3.5 cm and a thickness of 1 cm were placed in the streams for 3 years (2008 – 2011) where alkalinity, pH and major cation concentrations were measured periodically. The saturation indices of calcite (SIc) of stream water were −2.8±0.4 at site A, −2.5±0.4 at site B and –0.5±0.4 at site C. Annual weight loss ratio for tablets were extremely high at site A (0.11–0.14 mg cm^{-2} d^{-1}), high at site B (0.05 mg cm^{-2} d^{-1}), and low at site C (0.005 mg cm^{-2} d^{-1}). The contrasting rates of weight loss are mainly explained by chemical conditions of stream water. In addition, laboratory experiments for dissolution of limestone tablets using a flow-through apparatus revealed that flow conditions around the limestone tablet is another important factor for dissolution in the stream environment. These results revealed that limestone dissolves at a rapid rate where water unsaturated to calcite continuously flows, such as in an allogenic stream.

Key words: Karst, Limestone, Dissolution, Weathering experiment, Tablet, Stream flow

1. Introduction

Limestone plateaus with many dolines develop in karst terrains, especially in humid temperate regions such as Japan. One of the most important factors related to evolution of karst landform is denudation rate in various environments including ground surface, unsaturated soil, saturated soil and streams. The shallow weathered bedrock zone immediately beneath the soil-bedrock interface plays an important role in limestone dissolution and evolution of karst landforms (Williams, 1983). In typical karst terrains, however, limestone also dissolves in streams flowing around the margin of the plateau where stream water or groundwater is in direct contact with limestone. For example, an 'allogenic stream', a stream flowing from basins underlain by non-carbonate rocks, also makes a doline or other karst features (White, 1988; Ford and Williams, 2007). The impact of allogenic streams on landform evolution has not been well studied.

There are several techniques for estimating denudation rates of karst terrains. Chemical denudation rates in karst areas were classically estimated from Ca flux, i.e. average Ca ion concentrations and annual discharge from springs (e.g. Smith and Atkinson, 1976). For the case of a doline with an allogenic stream, however, estimating denudation rate from the Ca flux method has the following problems: (1) allogenic inputs are mixed with autogenic (on plateau) inputs during flow process in cave, and (2) caves immediately below dolines with allogenic stream are generally inaccessible.

The technique of field weathering experiments using a weight loss approach is an effective method for estimating the potential for dissolution under various environmental conditions (Trudgill, 1977; Jennings, 1981; Crabtree and Trudgill, 1985; Trudgill et al., 1994; Inkpen, 1995; Urushibara-Yoshino et al., 1999; Matsukura and Hirose, 1999; Dixon et al., 2001; Thorn et al., 2002, 2006; Plan, 2005; Matsukura et al. 2007; Yoshimura et al., 2009). The method is simple: installing a rock specimen with a known weight and surface area to a field site and measuring the weight loss after a period. The method also has problems that (1) the methodology itself may impact results of weathering rates (Inkpen, 1995) and (2) the estimated denudation rate for a short-term experiment (a few years) would be affected by temporal variation. However, this method enables us to directly estimate 'spatial variation' of limestone dissolution rate at any site. Past weathering experiments using this technique have focused on (1) topography (Crabtree and Trudgill, 1985 ; Plan, 2005), (2) duration (Trudgill et al., 1994), (3) climate (Urushibara et al., 1999), (4) difference between limestone and other rocks (Matsukura and Hirose, 1999; Thorn et al., 2002, 2006; Plan, 2005; Matsukura et al. 2007), and

(5) dissolution in caves (Yoshimura et al., 2009). Most of these experiments were conducted on the ground surface or in soil, but they did not particularly focus on dissolution in stream flow, including allogenic stream flow.

The present study focuses on the dissolution of limestone in stream flow along a margin of a karst plateau. The aim of the present study is to determine which environmental factors are significant for the dissolution under flowing water, based on a combined approach of field and laboratory experiments using limestone tablets and chemical analysis of the contact water.

2. Field Experiment

2.1. Study site

Field weathering experiments were conducted around a small karst plateau, 'Sendaihira', in the central Abukuma Mountains, Japan (Fig. 1), located in humid temperate region with humid summers and dry winters. The mean annual precipitation (1981–2010) at the nearest meteorological station 'Ono-niimachi' is 1245 mm, of which 71% falls from May to October. Mean monthly temperature ranges from −0.9 °C to 22.9 °C and the annual mean is 10.5 °C. The maximum depth of snow cover around the test sites reaches 20–30 cm in February. The vegetation around the sites is a combination of natural broad-leaved forest and planted forest of Japanese cedar, although grassland is artificially maintained around the top of the plateau. The underlying bedrock of the plateau is recrystallized massive limestone, which is in contact with shale layers at the eastern side and has a strike in the NNW–SSE direction with almost vertical dip (Ehiro et al., 1989). These sedimentary rocks are metamorphosed by Cretaceous granite, which outcrops to the southern and eastern margins. The age of these layers has not been determined precisely. An airborne LiDAR DTM with 2 m resolution reveals that two major active dolines have developed in a valley along the lithological boundary between limestone and shale (Fig. 1c). Two headwater streams originating from eastern hillslopes underlain by shale flow into both dolines, which are also connected to the two major caves beneath the karst plateau (Marui et al., 2003).

(Fig. 1)

2.2 Methods

85 We selected three sites of stream for field experiment (Fig. 2). Sites A and B are headwater streams flowing
86 into the dolines, and site C is located ~30 m downstream of a karst spring (Fig. 1c). Table 1 shows
87 hydrological and geomorphic conditions for the sites. Local channel gradient represents average gradient for a
88 50-m reach around each stream site. The gradient of site A is almost twice as that of site B. Channel
89 morphology at sites B and C is a 'pool' whereas site A is located in a 'rapid' section. Stream discharge
90 measured with a volumetric method varied from 90 $cm^3\ s^{-1}$ (site C) to 4900 $cm^3\ s^{-1}$ (site B) at base flow stages
91 (average of May 24, June 21, and July 21, 2008). We visually confirmed that these streams are perennial and
92 almost constant base flows continued even in cold, snowy winter season from the start to the end of the field
93 experiment. Although we could not make direct measurements on flow velocity due to shallowness or
94 slowness of the flow, we have estimated mean water flux from stream width, flow depth, and discharge at base
95 flow stage (Table 1). Water flux at site A is about 6.5 cm/s (depth of 2 ± 1 cm) which is slightly higher than at
96 site B (4.5 cm/s; depth of 10 ± 3 cm), and much higher than at site C (0.3 cm/s; depth of 10 ± 3 cm).
97
98 (Table 1)
99 (Fig. 2)
100 Limestone blocks for field experiment were taken near the Abukuma Cave, Fukushima Prefecture, which is
101 lithologically the same bedrock below the two dolines (sites A and B) and the upstream source of site C. The
102 limestone blocks which were used were uniform. The limestone blocks were cored and then sliced into
103 standard-sized tablets, which have a diameter of 34.5 mm, a thickness of 11.0±0.6 mm, a surface area of
104 30.60±0.37 cm^2, a weight of 27.2±1.2 g and a bulk density of 2.67±0.02 g cm^{-3}. The density of rock was
105 2.78±0.03 g cm^{-3}, and therefore, porosity was estimated to be 3.7±1.4%. X-ray fluorescence analysis by
106 Suzuki et al. (2000) showed that the limestone contains 55.5% of CaO, 0.22% of MgO, 0.19% of Al_2O_3, and
107 0.10% of $FeO+Fe_2O_3$.
108 We prepared a total of eight tablets for the field experiment. The surfaces of the tablets were polished with
109 carborundum #400. The tablets were weighed to an accuracy of 1 mg using a microbalance after oven drying
110 at 110 °C for 24 hours. We placed a nylon mesh bag (mesh size of 3.57 mm), in which a set of two tablets
111 were enclosed, at each stream site. The drawstrings of the mesh bags were fixed to tree trunks or branches
112 (Fig. 2). These tablets were collected about every six months and rinsed carefully with water in the laboratory.

113 Then the tablets were dried at 110 °C for 24 hours and reweighed. To evaluate the impacts of washing and
114 drying on dissolution rate, only washing and drying processes in the laboratory were simultaneously
115 performed for two 'control' tablets during the entire experimental period. The field experiment was conducted
116 for about 3 years from April 30, 2008 to May 3, 2011. The actual period of installation of tablets in the stream
117 flow was 1044 days, which is shorter than the whole period (1100 days) because the treatment in laboratory
118 was required for a total of 56 days. We also confirmed that the tablet bag at site C had moved out of the stream
119 flow during the last period by May 3, 2011. Therefore, we used the 863-day records until October 10, 2010 for
120 site C.
121 In order to understand chemical conditions of stream sites related to limestone weathering, we repeated *in situ*
122 measurement and sampling of stream water for a total of 21 times in the experimental period. The pH of
123 stream water was measured *in situ* with a portable glass electrode system (Horiba D-54) composed of an
124 Ag-AgCl internal electrode and 3.33 mol L^{-1} KCl solution. The temperature dependence of pH was
125 compensated automatically. The pH meter was calibrated using three standard solutions within 24 hours
126 before measurement. Although the system officially has an accuracy of ±0.02 for the observed pH range, the
127 fluctuation exceeds 0.02 during *in situ* measurement. We recorded a value of pH about 15 – 20 min after the
128 setting of the glass electrode to achieve a fluctuation of less than 0.05 within 5 min. Stream water was
129 sampled for alkalinity titration and ICP-AES analysis. Alkalinity was determined by titration to pH 4.8 using
130 0.01N H_2SO_4 and BCG-MR indicator using micro-pipettes at a 0.1 mL interval. The remaining original water
131 sample was filtered to 0.20 μm to measure concentrations of dissolved Ca, Mg, Si, K, and Na ions with
132 ICP-AES (Nippon Jarrell-Ash ICAP-757 from 2008 to 2010, Perkin Elmer Optima 7300DV from 2010 to
133 2011) at the Research Facility Center for Science and Technology in University of Tsukuba. The relative
134 standard deviation for Ca concentration was less than 2% except for two data in site A. We did not analyze
135 concentrations of other anions. Marui et al. (2003) reported that the stream water at sites A and B contains Cl
136 of 3 – 5 mg L^{-1}, SO_4 of 1 – 4 mg L^{-1}, NO_3 of 0 – 0.2 mg L^{-1} and PO_4 of 0 – 0.02 mg L^{-1} in August, 2001 and
137 February, 2002. The anion concentrations during the experiment would be at a similar level, since there were
138 no significant changes in land use and vegetation from 2001 to early 2011. Using all the measured chemical
139 parameters, we calculated saturation index for calcite (SIc), which is defined as logarithmic ratio of the ion
140 activity product over equilibrium constant for reaction of calcite dissolution (Ford and Williams, 2007). We

141 used the PHREEQC software with a geochemical database file of phreeqc.dat (ver 2.15.0) for calculation of
142 SIc (Parkhurst and Appelo 1999).
143
144 *2.3. Results*
145 We calculated two weathering rates for tablets: (1) mean rate of weight loss and (2) annual weight loss ratio,
146 (Table 2). The mean rate of weight loss is the total weight loss for each tablet divided by surface area and
147 experimental period, i.e. 1044 days for sites A/B and 863 days for site C. Weight loss of two control tablets
148 revealed that the washing and drying processes cause weight losses of 1.3±3.6 mg per one treatment. The
149 uncertainty for single measurement is about 4 mg. For the entire experimental period, six treatments give a
150 reduction of 7.5 mg, and five treatments (by 863 days at site C) give reduction of 6.3 mg. Therefore, the
151 observed weight loss is reduced by 7.5 mg for sites A and B and by 6.3 mg for site C. The mean daily rate of
152 weight loss varied from 0.005 mg cm^{-2} d^{-1} at site C (No. 9) to 0.137 mg cm^{-2} d^{-1} at site A (No. 18) (Table 2).
153 We also calculated annual weight loss ratio in order to compare the results of the other studies. The annual
154 weight loss ratio at site A was extremely high (4.5–5.7% a^{-1}), and exceeded any other annual weight loss ratio
155 reported in previous field experiments using limestone or dolomite tablets: 0.1–0.6% a^{-1} at Magnesian
156 Limestone hillslopes (Crabtree and Trudgill, 1985; Trudgill et al., 1994), 0.01–3.04% a^{-1} for dolomite at
157 Kärkevagge (Thorn et al. 2006), and 0.08–3.7% a^{-1} for the same limestone installed in granitic soil of
158 Abukuma Mountains (Matsukura et al., 2007; see Fig. 1b for location). The surface of tablets at site A had
159 been intensively affected by dissolution. For example, the surface of a tablet (No. 17) placed at site A was
160 more rugged than the tablets placed at site C or non-weathered polished limestone (Fig. 3).
161 (Table 2)
162 (Fig. 3)
163 All the chemical indices such as pH, alkalinity, and Ca concentration were higher at site C and lower at sites A
164 and B (Table 3). Annual average water temperature was almost the same (10–11°C). Saturation indices for
165 calcite (SIc) were low (–3 to –2) at both sites A and B, and high (about –0.5) at site C. Fig. 4 shows temporal
166 variation of pH and SIc. These indices of water chemistry have a weak seasonal variation, where both pH and
167 SIc increase in the fall and decrease in spring for all sites. The difference in SIc between sites is clearer than
168 the difference in pH. SIc of the stream water at site C was significantly greater than the other sites because

169 contrasts in alkalinity and Ca concentration are more obvious (Table 3). Stream water at site C sometimes
170 reached the state of saturation with respect to calcite (SIc ~ 0). In contrast, stream waters at sites A and B were
171 under-saturated (< –1) to calcite for the whole period. The observed contrasts between site C and the other
172 sites are explained by lithology of source area (Fig. 1). Stream water at site C originated from a karst spring
173 below the plateau which had already reacted with limestone through percolation into the plateau, while the
174 stream water at site A had no chance to be in contact with limestone in the upstream sources underlain by
175 shale. Although a part of drainage area for site B includes the limestone plateau, site B has a slightly higher
176 pH and SIc than site A (Table 3). The partial source of the limestone plateau is not likely to contribute to the
177 water chemistry at site B. The Welch's t-test revealed that the difference of average pH or SIc between sites A
178 and B is not statistically significant ($p > 0.05$). Therefore, sites A and B have similar chemical conditions in
179 terms of dissolution of calcite.

180 (Table 3)

181 (Fig. 4)

182 The difference in stream water chemistry, such as Sic, affects the mean rate of weight loss, particularly for the
183 case of site C where stream water is sometimes chemically saturated to calcite. However, there is a question
184 that the very high rates of weight loss at sites A and B can be explained by water chemistry alone. There is a
185 significant difference in flow conditions around tablets (Table 1, Fig. 2), and this may also contribute to the
186 difference in dissolution rate for these sites.

187

188 **3. Laboratory experiments**

189 *3.1. Experimental Design*

190 A laboratory experiment was carried out to test the effect of flow rate of stream water on dissolution of
191 limestone tablet. We employed a flow-through apparatus (Fig. 5). Distilled water in an input solution bottle
192 was infused into a 60-mL reaction bottle with a peristaltic pump at a constant flow rate, and the solution in the
193 reaction bottle was drained at the same rate simultaneously. This apparatus and a similar style one were also
194 used for an experiment to examine the dissolution of granodiorite tablets (Yokoyama and Matsuskura, 2006),
195 and to test the effect of calcite saturation of stream water on dissolution of limestone tablet (Hattanji et al.
196 2008). Three runs were conducted for 24 days at the three different flow rates of 100 mL d^{-1}, 550 mL d^{-1} and

197 4500 mL d^{-1}. For each run, one limestone tablet was inserted into the reaction bottle. We used the limestone
198 tablets with the same size and origins as those used in the field experiment. The reaction bottle was settled in
199 an incubator to keep the temperature at 20°C. Although the temperature was higher than average stream water
200 temperature (~10°C) at sites A – C, variation of several equilibrium constants (pK_1, pK_2, and pK_C) related to
201 the dissolution reaction series of calcite was less than 2% in this temperature range (Ford and Williams, 2007;
202 p.48, Table 3.6). Partial pressure values of CO_2 in laboratory atmosphere were constant at 0.05–0.06%. The
203 output solution drained from the reaction bottle was collected for chemical analysis including measurements
204 of pH, alkalinity and dissolved cation concentrations every two days. The analytical method is almost the
205 same as those in the field experiment. The same portable pH meter (Horiba D-54, an accuracy of ± 0.02) was
206 used for measurement of pH. Alkalinity was determined by titration to pH 4.8 using 0.01N H_2SO_4 and
207 BCG-MR indicator using micro pipettes at a 0.1 mL interval. The dissolved Ca, Mg, Si, K, and Na ions were
208 measured with ICP-AES (Perkin Elmer Optima 7300DV).

209 (Fig. 5)

210

211 *3.2. Results*

212 We calculated two parameters representing weathering rates: (1) mean rate of weight loss and (2) dissolution
213 rate of calcite. Again, mean rate of weight loss is total weight loss of each tablet divided by surface area and
214 the experimental period, i.e. 24 days. The daily mean rate of weight loss varied from 0.037 mg cm^{-2} d^{-1} for
215 run 1 to 0.124 mg cm^{-2} d^{-1} for run 3 (Table 4). However, duration of laboratory experiment is shorter than that
216 of the field experiment, and therefore total amount of weight loss is much smaller (< 100 mg).

217 (Table 4)

218 The second approach calculates 'dissolution rate of calcite' based on concentration of Ca ion for input and
219 output solutions. For all the runs, the output solution had higher Ca concentration than its input solution, and
220 loss of Ca from the tablet can be estimated from the increments of Ca concentration. Cumulative loss of Ca
221 from a tablet by the *n*th day, W_n (mg), is:

222 $$W_n = \sum_{i=1}^{n} ([Ca^{2+}]_{OUTi} - [Ca^{2+}]_{INi}) \cdot \rho v_i \qquad (1)$$

223 where $[Ca^{2+}]_{OUTi}$ is concentration of Ca ion in the output solution on the *i*th day in ppm (mg kg^{-1} solution),

224 $[Ca^{2+}]_{INi}$ is concentration of Ca ion in the input solution on the *i*th day in ppm (mg kg^{-1} solution), v_i is volume
225 of the output solution on the *i*th day in litre, and ρ is density of solution (= 1 kg L^{-1}). We estimated the
226 dissolution rate of Ca using the slope of regression line for the temporal increase of W_n. Assuming that all the
227 increments in the concentration of Ca ion are originated from the dissolution of calcite ($CaCO_3$) on the surface
228 of limestone tablet, we can convert dissolution rate of Ca into dissolution rate of calcite using weight ratio of
229 calcite to Ca (100/40). The calculated dissolution rate of calcite per unit surface area ranged from 0.018 to
230 0.098 mg cm^{-2} d^{-1} (Table 4).
231 Both dissolution rate of calcite and mean rate of weight loss increased with increasing flow rate (Fig. 6). This
232 result indicates that flow rate is a significant controlling factor on dissolution and weathering of limestone
233 tablet. Although the SIc of output solutions were very low (< – 3) for all the runs, the solution in the reaction
234 bottle indicated higher SIc values, ranging from −3.5 to −0.61 (Table 4). For the case of the lowest flow rate
235 (run 1), the solution remaining in the reaction bottle was not completely saturated but close to saturation (SIc
236 = −0.61). The slower flow rate allows development of a thicker boundary layer with higher pH and Ca
237 concentrations, which, in turn, restricts fast dissolution. For the case of the highest flow rate (run 3) with low
238 SIc (−3.5), faster circulation enhanced the dissolution of tablet.
239 The mean rate of weight loss was 0.02–0.03 mg cm^{-2} d^{-1} higher than dissolution rate of calcite calculated from
240 water chemistry analysis (Fig. 6 and Table 4). The factors responsible for this inconsistency would be: (1) the
241 effect of physical detachment of vulnerable parts, such as the edge or rough surface, during drying and
242 weighing process, (2) removal of 'diffusion boundary layer' (Ford and Williams, 2007) surrounding the tablet
243 surface before weighing, which contains more amounts of dissolved Ca, and (3) errors in measurement or
244 analysis. Accumulation of errors in ICP-AES analysis was only 0.002 mg cm^{-2} d^{-1} for the greatest case of run
245 3. Although the errors in weight measurement (±4 mg) are equivalent to 5–20% of total measured weight loss,
246 these are much smaller than the systematic difference between two measurements (Fig. 6). These facts imply
247 that effect of physical detachment and removal of a boundary layer are possible reasons for the inconsistency.
248 For these cases, mean rate of weight loss would approach the value of 'dissolution rate of calcite' if the
249 laboratory experiment was to continue for a duration as long as the field experiment.
250 (Fig. 6)
251

252

253 **4. Discussion**

254 *4.1. Field weathering rates vs dissolution rates in the laboratory*

255 We compared the results of field experiment with laboratory experiment, in order to understand what controls
256 the dissolution of limestone in streams around a karst plateau. Rates of weight loss or dissolution rates of
257 calcite were plotted against saturation indices for calcite (SIc, Fig. 7a) or pH (Fig. 7b) of stream water for field
258 experiment or output solutions for laboratory experiment. For laboratory runs, the SIc values for output
259 solutions were used here as a reference, which represents flowing water outside of the diffusion boundary
260 layer developed on tablet surface. The results of laboratory experiment by Hattanji et al. (2008) were also
261 plotted in Fig. 7, in which the effect of calcite saturation of circulating water on limestone dissolution was
262 tested using the same apparatus and the same-sized limestone tablets. The runs were conducted at a constant
263 flow rate of 63±2 mL d^{-1} and continued for 23 days with various input solutions with different SIc.
264 Dissolution rate of calcite was similarly calculated using Eq. (1).

265 (Fig. 7)

266 In Fig. 7a, the field rate at site C, which represents a flow from a karst spring, show a good fit with the data of
267 Hattanji et al. (2008) at the near equilibrium solution. The result ensures that slower rate of weight loss at site
268 C is well explained by water chemistry, in other words, the near equilibrium state of flowing water. In contrast,
269 dissolution rates and mean rates of weight loss were scattered for lower SIc (–3 to –2). Sites A and B have
270 about 10 times higher weathering rates of laboratory run 1 or the data of Hattanji et al. (2008), even under
271 similar chemical conditions of flowing water.

272 Dissolution rates vary from 0.018 mg cm^{-2} d^{-1} (run 1) to 0.098 mg cm^{-2} d^{-1} (run 3) for the laboratory
273 experiment, or even to 0.10–0.14 mg cm^{-2} d^{-1} for the field experiment within this narrow range of pH
274 (6.5–7.1). Laboratory dissolution rate for the highest flow rate (run 3) is similar to the field rate of weight loss
275 at site A where faster stream flow in a rapid stream morphology would enhance the reaction process on the
276 surface of a tablet (Table 1 and Fig. 2a). Although there are significant differences in SIc between these
277 laboratory and field data (Fig. 7a), the ranges of pH in the output solution for all runs are slightly less than the
278 pH of stream water at sites A and B (Fig. 7b). These facts indicate that the very high dissolution rates at sites A
279 and B are explained by combination of stream water chemistry and high flow velocity around a tablet.

280 The results of our field and laboratory experiments support the interpretation that transport of ions around the
281 tablet is important in dissolution of limestone in the field environment. Morse and Arvidson (2002), who
282 summarized the results of numerous laboratory experiments on calcite dissolution, indicated that dissolution
283 rates are controlled by transport of H^+ for low pH condition (pH < 4), and then turn to depend on surface
284 reaction at the state of near equilibrium. For the latter case, dissolution rate decreases with increasing SIc near
285 equilibrium state (Rickard and Sjöberg, 1983), which actually fits well with the results of Hattanji et al. (2008).
286 Agreement of field and laboratory dissolution rates at a higher flow rates implies that transport control
287 predominates in dissolution process at these sites even under neutral pH (6–7). Indeed, Takaya et al. (2006)
288 conducted a series of laboratory experiments on the dissolution of limestone blocks in distilled water using a
289 closed system, and confirmed that transport control prevails in distilled water for limestone block samples.
290
291 *4.2. Implications for landscape evolution*
292 The result of the present study implies an important role of allogenic streams on landscape evolution in karst
293 terrains. Exposed limestone will be dissolved at a high rate where unsaturated water flows rapidly such as in
294 sites A and B. For the case of Sendaihira plateau in Abukuma Mts. (Fig. 1), stream flow originating from small
295 basins underlain by shale enhances rapid dissolution of limestone on the eastern side of the plateau. The
296 potential denudation rates around sites A and B can be estimated from the observed mean rate of weight loss
297 of tablets combined with surface area and bulk density of tablets. Assuming the surface area of 30.6 cm^2 and
298 bulk density of 2.67 g cm^{-3} for each limestone tablet, estimated chemical denudation rates are equivalent to
299 150–187 mm ka^{-1} for site A and 71–72 mm ka^{-1} for site B. These rates are much faster than the denudation
300 rates measured at the top of karst terrain. Matsushi et al. (2010) reported denudation rates of 20–43 mm ka^{-1}
301 for pinnacles on the top of the Sendaihira plateau (Fig. 1c). Another field experiment in the Abukuma area
302 (Matsukura et al., 2007, see Fig.1b for location) reported a slower rate of weight loss (0.098% a^{-1}) in
303 unsaturated granitic soil, which is equivalent to the denudation rate of only 3.4 mm ka^{-1}. The contrast of
304 denudation rates on the hill top and potential rates at the eastern side of plateau should enhance the
305 topographic contrast in time scales for landscape evolution (> 100 ka), although climatic change must alter
306 hydrological and chemical conditions of stream flow, and the estimated rates must vary with time to some
307 extent. Further discussion on the effect of allogenic stream on landscape evolution will be a future issue.

5. Conclusion

The present study focused on the dissolution of limestone in stream flow around a limestone plateau. In the field experiment, limestone tablets were installed in three sites (A – C) of stream from 2008 to 2011. Field rate of tablet weight loss was extremely high (0.11–0.14 mg cm^{-2} d^{-1}) at the high-gradient stream site A with non-carbonate sources, high (0.05 mg cm^{-2} d^{-1}) at the low-gradient site B with non-carbonate sources, and low (0.005 mg cm^{-2} d^{-1}) at the low-gradient site C with karst sources. The slowest dissolution rate was observed in the stream with a karst spring (site C) where the stream water is close to saturation to calcite (SIc ~ –0.5), thus the chemical condition of stream water is the primary control on dissolution rate. The high dissolution rates at sites A and B are not only explained by chemical conditions of stream water, but also high velocity of water flow around the tablets. The laboratory dissolution rate for the case of the highest flow rate is equivalent to the highest field rate of tablet weight loss at site A. The results of our field and laboratory experiments revealed that limestone dissolves at a fast rate where continuous unsaturated water travels a relatively fast around tablet, such as in an allogenic stream. This fact implies that an allogenic stream, i.e. stream flow from non-limestone sources, has a strong impact on the local denudation of limestone and evolution of karst landscape.

Acknowledgements

This study is financially supported by the Science Research Fund of the JSPS (19300305) through Matsukura. The airborne LiDAR DTM provided by Kokusai Kogyo Co. Ltd. is used as the CSIS Joint Research (403). We thank Dr. Iona Dias for her technical support to improve the manuscript, and two anonymous reviewers for their constructive comments and suggestions, which improved the earlier version of the manuscript.

References

Crabtree, R. W., Trudgill, S. T., 1985. Chemical denudation on a Magnesian Limestone hillslope, field evidence and implications for modelling. Earth Surface Processes and Landforms 10, 331– 341.

Dixon, J. C., Thorn, C. E., Darmody, R. G., Schlyter, P., 2001. Weathering rates of fine pebbles at the soil surface in Kärkevagge, Swedish Lapland. Catena 45, 273–286.

336 Ehiro, M., Kanisawa, S., Taketomi, Y., 1989. Pre-Tertiary Takine Group in the central Abukuma Massif.
337 Bulletin of the Fukushima Museum 3, 21–37 (in Japanese).
338 Ford, D., Williams, P., 2007. Karst Hydrology and Geomorphology.Wiley, Chichester, UK.
339 Hattanji T., Yamamoto, M., Matsukura, Y., 2008. Dissolution rates of limestone tablets in a flow-through
340 system: A laboratory experiment. Tsukuba Geoenvironmental Sciences 4, 3–7.
341 Inkpen, R., 1995. Errors in measuring the percentage dry weight change of stone tablets. Earth Surface
342 Processes and Landforms 20, 783–793.
343 Jennings, J. N., 1981. Further results from limestone tablet experiments at Cooleman Plain. Australian
344 Geographical Studies 19, 224–227.
345 Marui, A., Hayashi, T., Kikuchi, M., Yamauchi, T., 2003. Hydrological environment of Abukuma Cave system.
346 Journal of Japanese Association of Hydrological Sciences 33, 71–84 (in Japanese, with English Abstr.).
347 Matsukura, Y., Hirose, T., 1999. Five-year measurement of weight loss of rock tablets due to weathering on a
348 forested hillslope of a humid temperate region. Engineering Geology 55, 69–76.
349 Matsukura, Y., Hattanji, T., Oguchi, C. T., Hirose, T., 2007. Ten year measurement of weight-loss of rock
350 tablets due to weathering in a forested hillslope of a humid temperate region. Zeitschrift für
351 Geomorphology N.F. 51, Supplementary Issue 1, 27–40.
352 Matsushi Y., Sasa K., Takahashi T., Sueki K., Nagashima Y., Matsukura Y., 2010. Denudation rates of
353 carbonate pinnacles in Japanese karst areas: estimates from cosmogenic ^{36}Cl in calcite. Nuclear
354 Instruments and Methods in Physics Research B 268, 1205–1208.
355 Morse, J., W. and Arvidson, R. S., 2002. The dissolution kinetics of major sedimentary carbonate minerals.
356 Earth Science Reviews 58, 51–84.
357 Parkhurst, D. L., Appelo, C. A. J., 1999. User's guide to PHREEQC (Version 2) – A computer program for
358 speciation, batch-reaction, one-dimensional transport, and inverse geochemical calculations. U. S.
359 Geological Survey Water-Resources Investigations Report 99–4259, Denver, CO.
360 Plan, L., 2005. Factors controlling carbonate dissolution rates quantified in a field test in the Austrian Alps.
361 Geomorphology, 68, 201–212.
362 Rickard, D. T., Sjöberg, E. L., 1983. Mixed kinetic control of calcite dissolution rates. American Journal of
363 Science 283, 815–830.

364 Smith, D. I., Atkinson, T.C., 1976. Process, landforms and climate in limestone regions. In: Derbyshire, E. D.
365 (Ed.), Geomorphology and Climate, Wiley, New York, pp. 367–409.
366 Suzuki, M., Takaya, Y., Matsukura, Y., 2000. Dissolution experiment of limestone tablets. Bulletin of the
367 Terrestrial Environment Research Center, University of Tsukuba 1, 19–26 (in Japanese).
368 Takaya, Y., Hirose, T., Aoki, H., Matsukura, Y., 2006. Dissolution characteristics of limestone in laboratory
369 experiments. Journal of Geography (Japan) 115, 136–148 (in Japanese, with English Abstr.).
370 Thorn, C. E., Darmody, R. G., Dixon, J. C., Schlyter, P., 2002. Weathering rates of buried machine-polished
371 rock disks, Kärkevagge, Swedish Lapland. Earth Surface Processes and Landforms 27, 831–845.
372 Thorn, C.E. Dixon, J. C., Darmody, R. G., Allen, C. E., 2006. Ten years (1994–2004) of 'potential' weathering
373 in Kärkevagge, Swedish Lapland. Earth Surface Processes and Landforms 31, 992–1002.
374 Trudgill, S. T., 1977. Problems in the estimation of short-term variations in limestone erosion processes. Earth
375 Surface Processes 2, 251–256.
376 Trudgill, S. T., Crabtree, R. W., Ferguson, R. I., Ball, J., Gent, R., 1994. Ten year remeasurement of chemical
377 denudation on a Magnesian Limestone hillslope. Earth Surface Processes and Landforms 19, 109–114.
378 Urushibara-Yoshino, K., Kashima, N., Enomoto, H., Kuramoto, T., Miotoke, F. D., Nakahodo, T., Higa,
379 M.,1999. Secular change and regional differences of limestone solution rates in Japan. Journal of
380 Geography (Japan) 108, 45–58 (in Japanese, with English Abstr.).
381 White, W. B., 1988. Geomorphology and Hydrology of Karst Terrains. Oxford University Press, New York.
382 Williams, P.W., 1983. The role of the subcutaneous zone in karst hydrology. Journal of Hydrology 61, 45–67.
383 Yokoyama, T., Matsukura, Y., 2006. Field and laboratory experiments on weathering rates of granodiorite:
384 Separation of chemical and physical processes. Geology 34, 809–812.
385 Yoshimura, K., Fujikawa, M, Ishida, M., Kurisaki, K., Aizawa, J., 2009. Cave wall erosion near the entrance
386 to Akiyoshi-do Cave, Yamaguchi, Southwestern Japan. Journal of Speleological Society of Japan 34,
387 38–46.
388
389

390 *Captions*

391 Fig.1 Location and geologic map of the study area (A, B) and relief shading map using LiDAR DTM with
392 2 m resolution around the study sites (C). Contour interval of Fig. 1b is 20 m. In Fig. 1c, the white broken
393 line shows the margin of limestone exposure, and the broken lines with black arrows indicate the connection
394 between dolines and caves proven by Marui et al. (2003).

395

396 Fig. 2 Stream sites for the field experiment. Direction of stream flow is indicated with an arrow. A mesh
397 bag with two limestone tablets is indicated with a circle for each site.

398

399 Fig. 3 Surface of the limestone tablets installed at sites A, B and C after the experiment and surface of a
400 non-weathered polished limestone (D). All photographs were taken with magnification of 20×.

401

402 Fig. 4 Temporal variation of pH (A) and saturation index with respect to calcite (SIc, B) for stream water.
403 Daily rainfall was recorded at Ono-niimachi nearby the investigation sites.

404

405 Fig. 5 A flow-through apparatus using a peristaltic pump for the laboratory experiment. Distilled water in
406 an input solution bottle is infused into a 60-mL reaction bottle, in which one limestone tablet is placed.

407

408 Fig. 6 Effects of water flow rate on dissolution rate of calcite or rate of weight loss for limestone tablet.
409 The uncertainty is not shown if it is smaller than the size of plot itself.

410

411 Fig. 7 Comparison of field and laboratory weathering experiments. (A) Relationship between saturation
412 index for calcite (SIc) and weathering rates, (B) relationship between pH and weathering rates. Data from
413 Hattanji et al. (2008) shows the results of a similar laboratory experiment at a flow rate of 63 mL d^{-1} using
414 limestone tablets under different initial solutions.

415

416 Table 1 Hyrdological and geomorphic conditions for the sites of field weathering experiment

	Site A	Site B	Site C
Lithology of source area	shale	shale, partly limestone	limestone
Local channel gradient [m m^{-1}]	0.15	0.08	0.04
Drainage area [km^2]	0.062	0.321	0.071*
Stream width at base flow [m]	0.3	1.0	0.3
Discharge at base flow [cm^3 s^{-1}]	390 ± 40	4900 ± 1400	86 ± 43
Estimated water flux [cm s^{-1}]	6.5 ± 4.0	4.9 ± 2.2	0.3 ± 0.2
Channel morphology	rapid	pool	pool

417 *the estimated drainage area for site C is a reference value based on surface topography because groundwater
418 flow system of this karst plateau is unknown.

419 Table 2 Weight loss of tablets in the field experiment

	Site A		Site B		Site C	
Tablet No.	17	18	8	23	9	21
Measured weight loss [g]*	3.530	4.366	1.672	1.666	0.133	0.151
Net weight loss [g]*	3.523	4.359	1.665	1.659	0.128	0.145
Mean rate of weight loss [mg cm^{-2} d^{-1}]**	0.109	0.137	0.052	0.053	0.005	0.006
Annual weight loss ratio [% a^{-1}]***	4.47	5.72	2.14	2.17	0.19	0.23

420 *Uncertainty is 0.004 g for measured weight loss, and 0.005 g for net weight loss.

421 **Relative errors are 2.3% for tablets in sites A and B, 4.2–4.6% for site C.

422 ***Relative errors are 0.7% for all tablets.

423 Table 3 Chemical conditions of stream water in the field experiment. The data is an average of 21
424 measurements, and the standard deviation of measurements is shown as an error.

	Site A	Site B	Site C
pH	6.96 ± 0.35	7.14 ± 0.37	7.40 ± 0.33
alkalinity [meq kg^{-1}]	0.32 ± 0.04	0.33 ± 0.04	2.01 ± 0.24
Ca^{2+} conc. [mg kg^{-1}]	3.2 ± 0.7	3.3 ± 0.6	42.2 ± 5.8
SIc	−2.8 ± 0.4	−2.5 ± 0.4	−0.48 ± 0.36

425

426 Table 4 Dissolution rate and rate of weight loss for limestone tablets in the laboratory experiment

	Run #1	Run #2	Run #3
Flow rate [mL d^{-1}]	98 ± 2	553 ± 21	4510 ± 150
Tablet weight before the run [g]	26.266	24.874	25.151
Tablet weight after the run [g]	26.239	24.821	25.062
Weight loss of tablet [mg]	27 ± 5	53 ± 5	89 ± 5
Mean rate of weight loss [mg cm^{-2} d^{-1}]*	0.037 ± 0.002	0.075 ± 0.004	0.124 ± 0.007
Dissolution rate of calcite [mg cm^{-2} d^{-1}]**	0.018	0.056 ± 0.001	0.098 ± 0.002
Average pH for output water	6.96 ± 0.12	6.85 ± 0.14	6.47 ± 0.16
Average SIc for output water***	−3.1± 0.2	−3.8 (+0.3, −0.5)	−5.0 (+0.4, −1.4)
SIc in the reaction bottle at the end***	−0.61 ± 0.2	−1.6 ± 0.2	−3.5 (+0.4, −1.9)

427 *mean rate of weight loss during the 24-day experiment.

428 **dissolution rate calculated from the temporal increase of W_n. The error is not shown if it is < 0.001.

429 ***The asymmetric uncertainties shown in the parentheses are originated from errors of low alkalinity < 0.1

430 meq kg^{-1}.

431

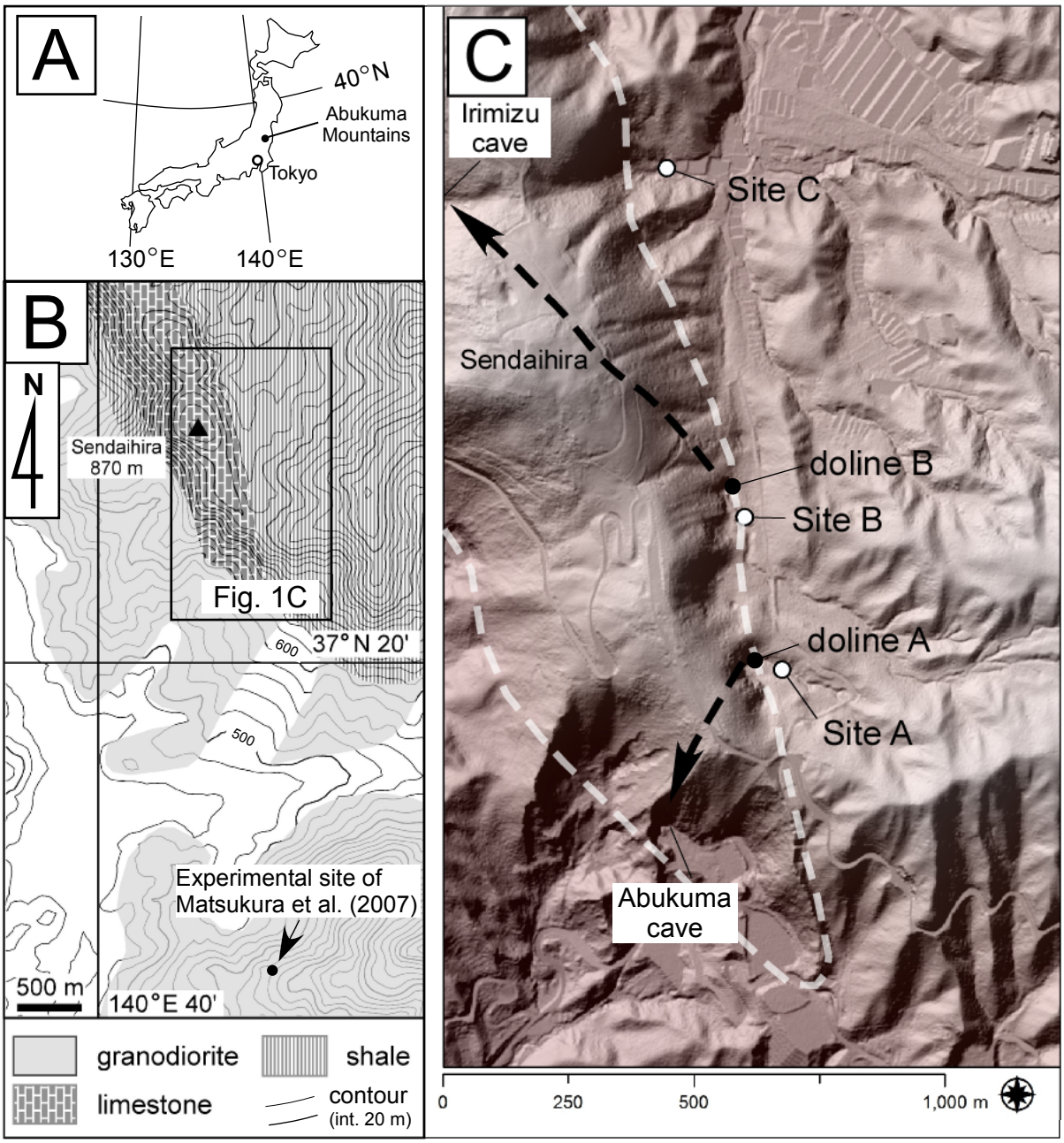
A
40°N
Abukuma
Mountains
Tokyo
130°E
140°E
B
N
Sendaihira
870 m
Fig. 1C
37° N 20'
600
500
Experimental site of
Matsukura et al. (2007)
500 m
140°E 40'
granodiorite
shale
limestone
contour
(int. 20 m)
C
Irimizu
cave
Site C
Sendaihira
doline B
Site B
doline A
Site A
Abukuma
cave
0
250
500
1,000 m

Figure 1

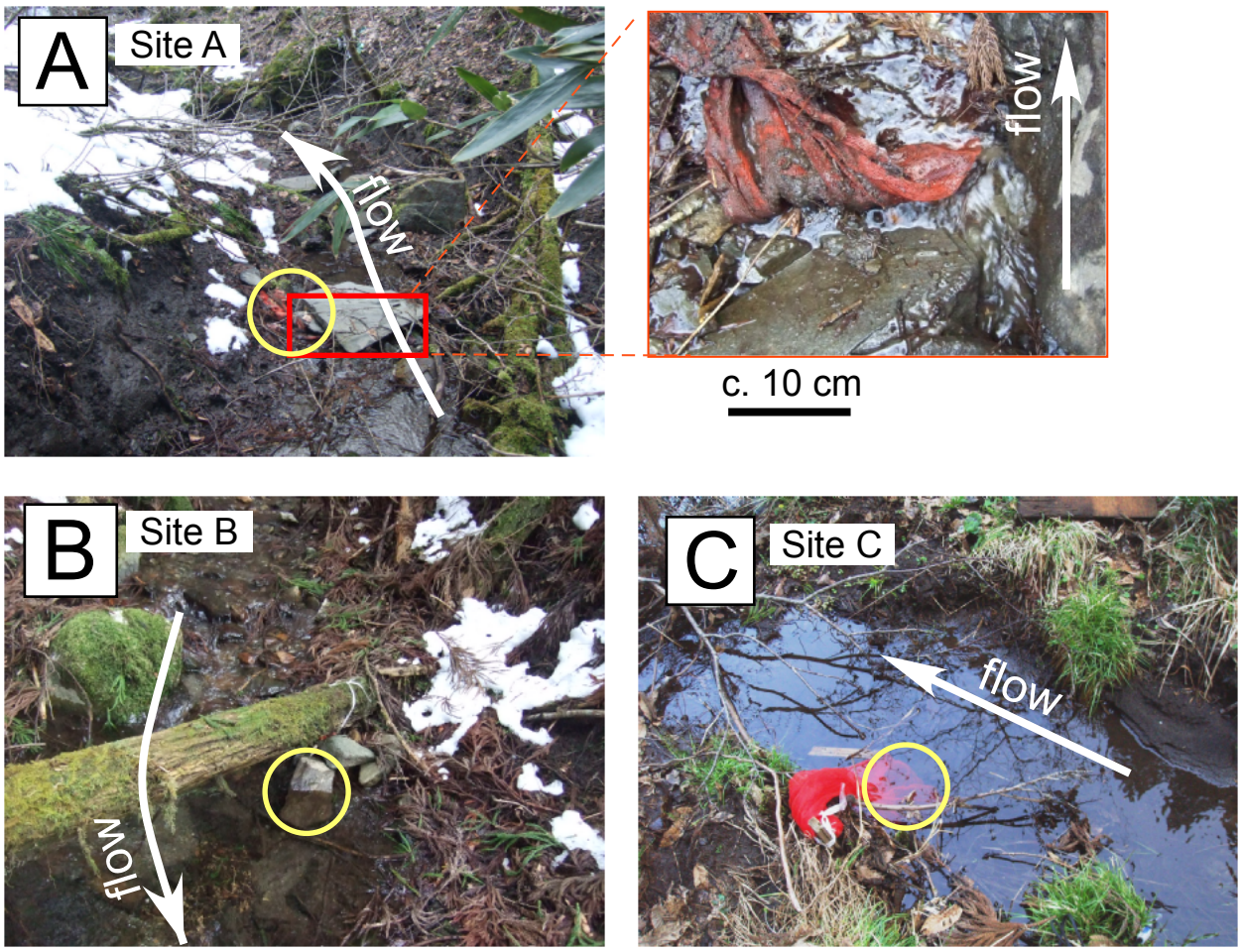

Figure 2

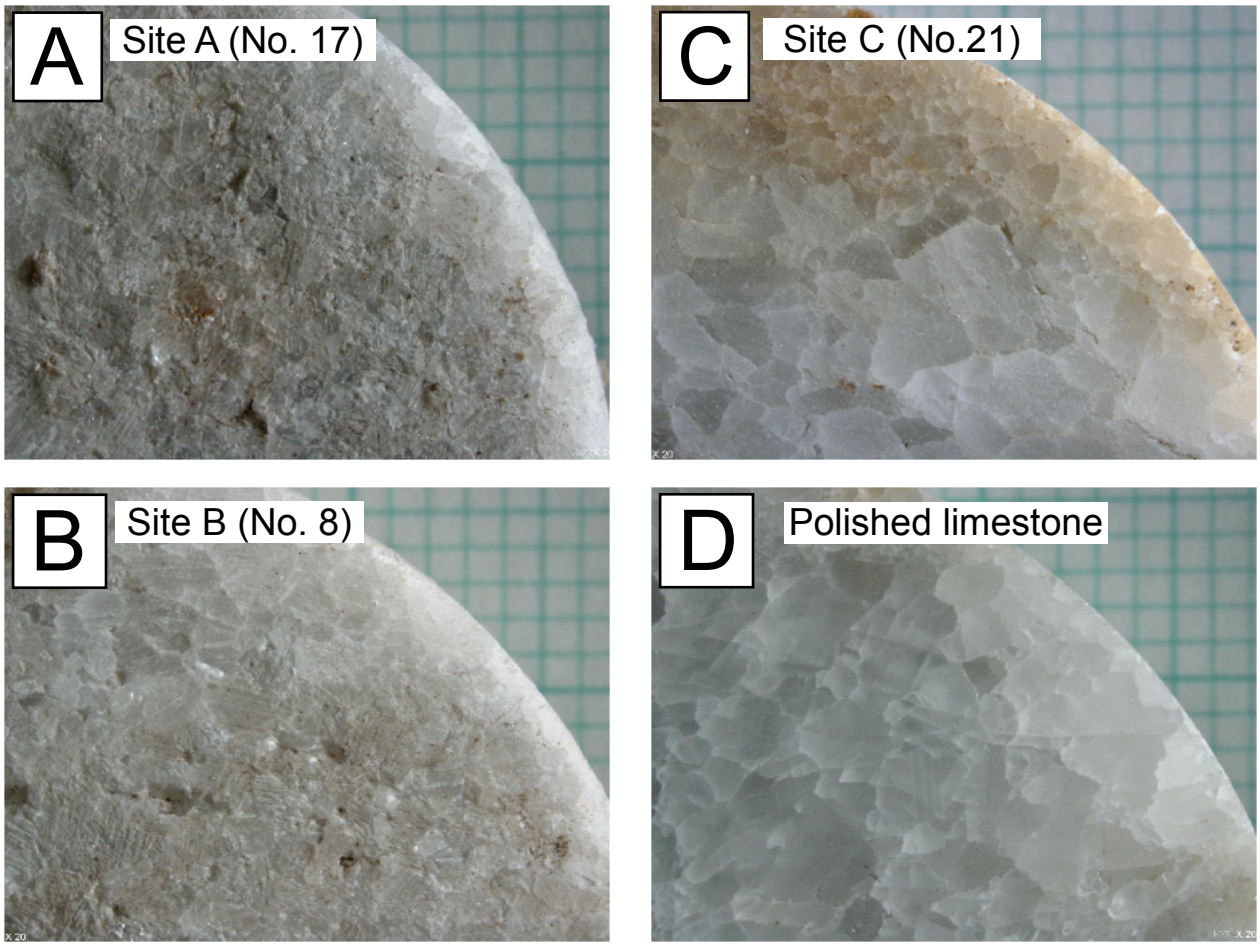

Figure 3

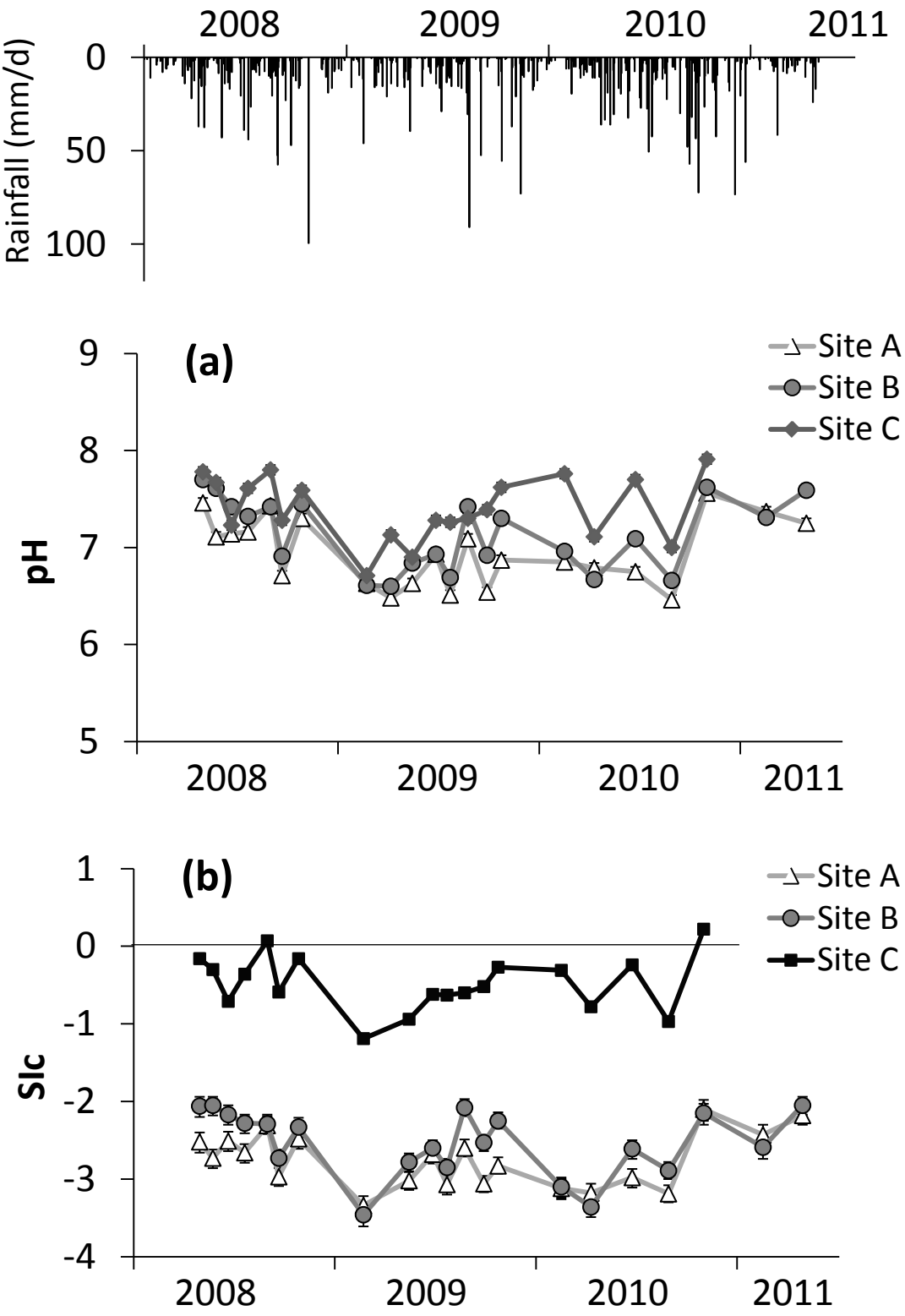
2008
2009
2010
2011
Rainfall (mm/d)
0
50
100
(a)
Site A
Site B
Site C
pH
9
8
7
6
5
2008
2009
2010
2011
(b)
Site A
Site B
Site C
SIc
1
0
-1
-2
-3
-4
2008
2009
2010
2011

Figure 4

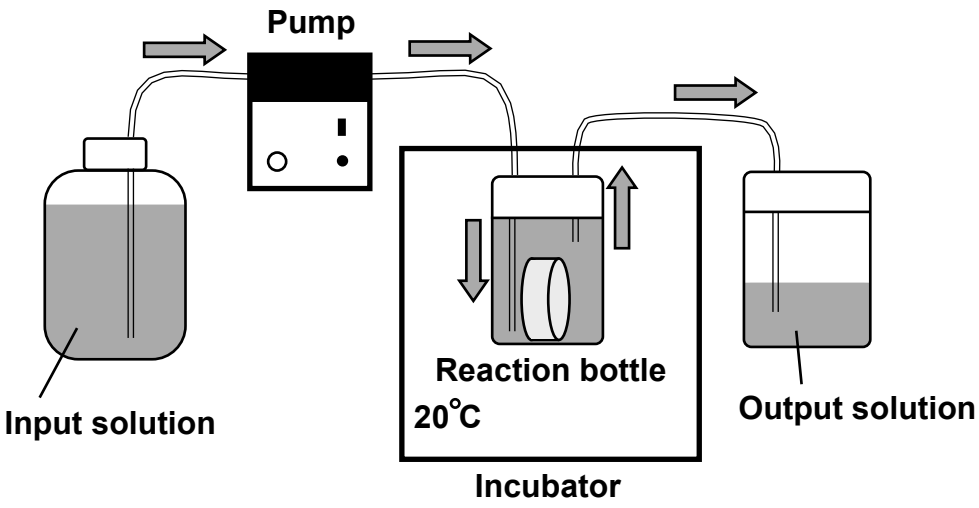
Pump
Input solution
Reaction bottle
20℃
Incubator
Output solution

Figure 5

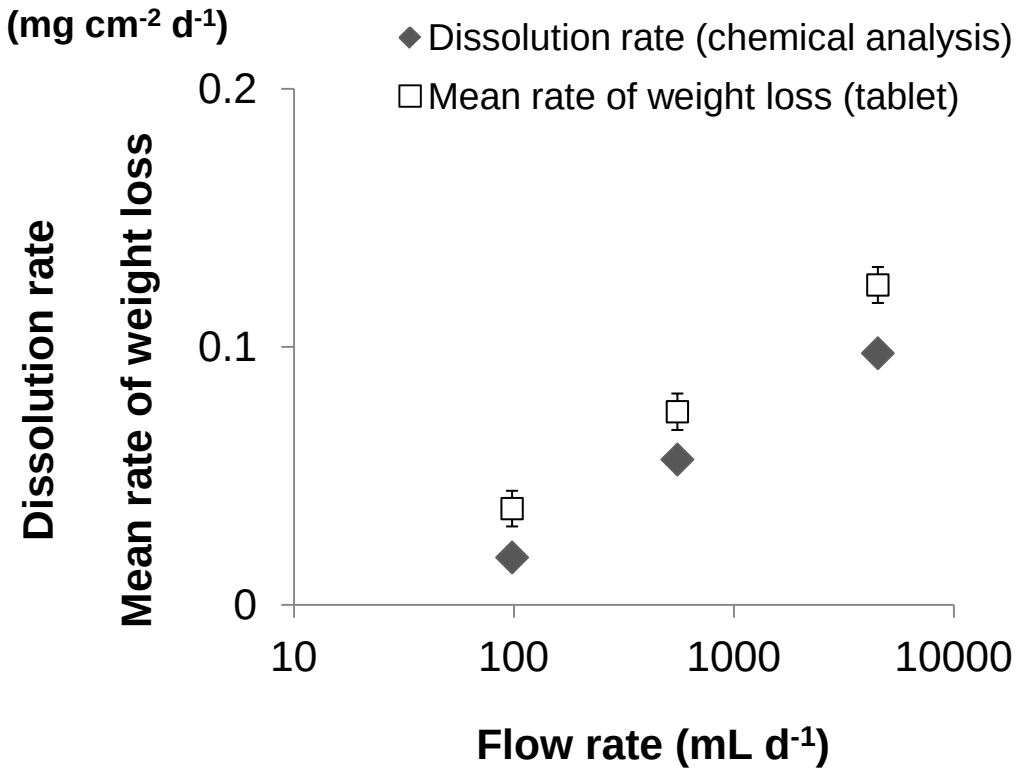
(mg cm-2 d-1)
Dissolution rate (chemical analysis)
Mean rate of weight loss (tablet)
Dissolution rate
Mean rate of weight loss
0.2
0.1
0
10
100
1000
10000
Flow rate (mL d-1)

Figure 6

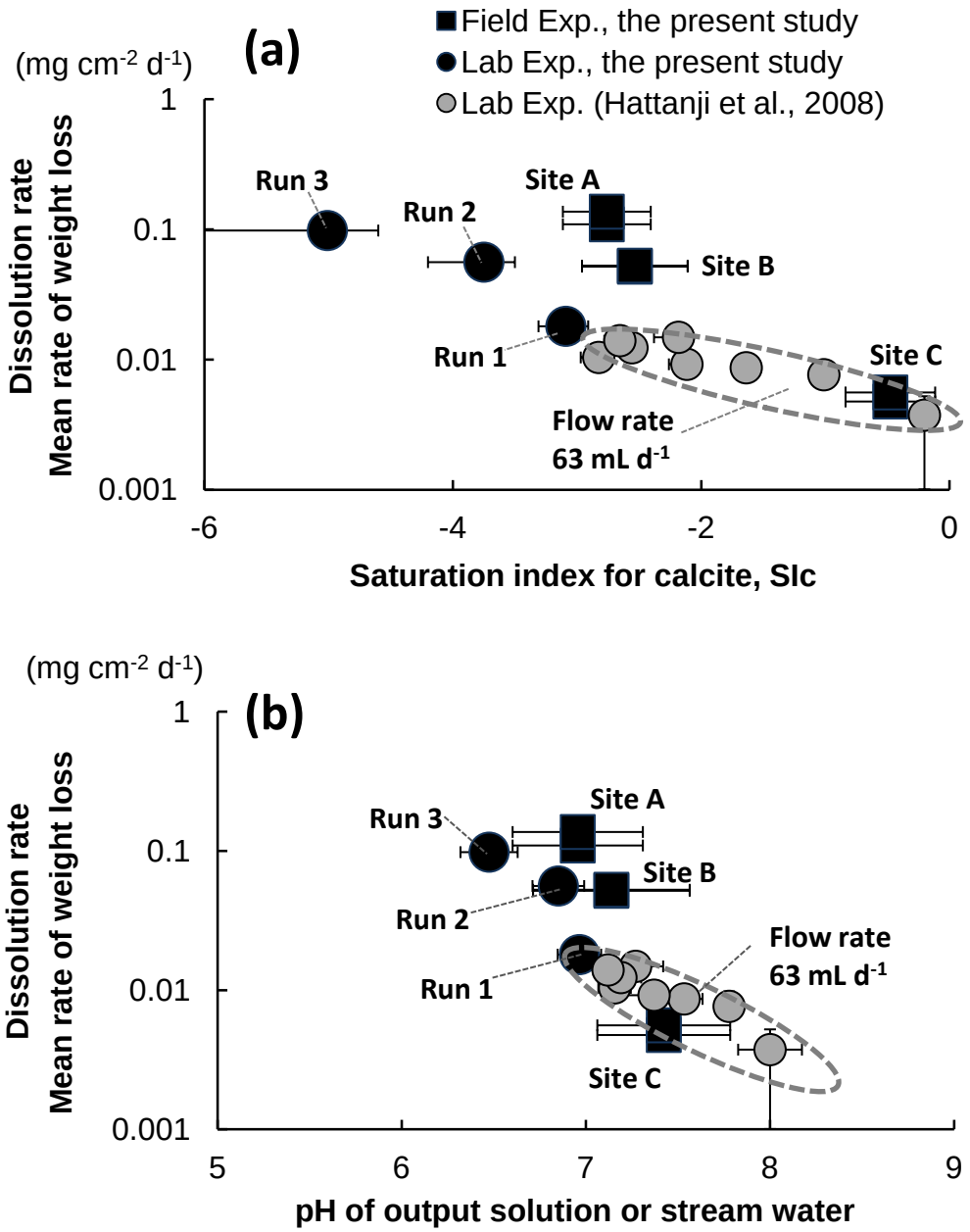
(a)
Field Exp., the present study
Lab Exp., the present study
Lab Exp. (Hattanji et al., 2008)
(mg cm-2 d-1)
Dissolution rate
Mean rate of weight loss
1
0.1
0.01
0.001
Run 3
Run 2
Site A
Site B
Run 1
Site C
Flow rate
63 mL d-1
-6
-4
-2
0
Saturation index for calcite, SIc
(b)
(mg cm-2 d-1)
Dissolution rate
Mean rate of weight loss
1
0.1
0.01
0.001
Run 3
Site A
Site B
Run 2
Flow rate
63 mL d-1
Run 1
Site C
5
6
7
8
9
pH of output solution or stream water

Figure 7